
Imaging in Random Media

George Papanicolaou

Department of Mathematics, Stanford University

<http://math.stanford.edu/>

Lectures IX and X

Coherent interferometry for imaging in random
media

Kirchhoff or travel time migration

Assume that the background velocity is known. Denote the deterministic background Green's function by $\hat{G}_0(\mathbf{x}, \mathbf{y}, \omega) = \frac{e^{i\omega\tau(\mathbf{x}, \mathbf{y})}}{4\pi|\mathbf{x} - \mathbf{y}|}$. We can then use the following imaging functional for the reflectivity $\rho(\mathbf{y}^S)$:

$$I^{KM}(\mathbf{y}^S) = \sum_{\mathbf{x}_S, \mathbf{x}_R} P(\mathbf{x}_R, \mathbf{x}_S, \tau(\mathbf{x}_S, \mathbf{y}^S) + \tau(\mathbf{y}^S, \mathbf{x}_R))$$

Here $\tau(\mathbf{x}, \mathbf{y}) = |\mathbf{x} - \mathbf{y}|/c_0$ is the travel time from \mathbf{x} to \mathbf{y} when the speed of propagation is c_0 .

This does not work in clutter because the deterministic travel time cannot deal with the delay spread in the traces. The delay spread is due to the scattering from the random inhomogeneities.

Incoherent Interferometry

Delay spread manifests itself in the frequency domain as random phases. To avoid this random phase problems in Kirchhoff migration imaging we mimic physical time reversal by computing cross-correlations of data traces, the **interferograms**, and summing

$$I^{INT}(\mathbf{y}^S) = \sum_{\mathbf{x}_r, \mathbf{x}_{r'}} P(\mathbf{x}_r, \cdot) *_t P(\mathbf{x}_{r'}, -\cdot) |_{\tau(\mathbf{x}_r, \mathbf{y}^S) - \tau(\mathbf{x}_{r'}, \mathbf{y}^S)}$$

The interferograms are given by

$$P(\mathbf{x}_r, \cdot) *_t P(\mathbf{x}_{r'}, -\cdot)(t) = \int_{-\infty}^{\infty} P(\mathbf{x}_r, s) P(\mathbf{x}_{r'}, s - t) ds$$

In the frequency domain we have

$$I^{INT}(\mathbf{y}^S) = \int d\omega \left| \sum_{\mathbf{x}_r} \hat{P}(\mathbf{x}_r, \omega) e^{-i\omega\tau(\mathbf{x}_r, \mathbf{y}^S)} \right|^2$$

Incoherent interferometry II

In the frequency domain we have

$$I^{INT}(\mathbf{y}^S) = \int d\omega \left| \sum_{\mathbf{x}_r} \hat{P}(\mathbf{x}_r, \omega) e^{-i\omega\tau(\mathbf{x}_r, \mathbf{y}^S)} \right|^2$$

This is almost **Matched Field Imaging**

$$I^{MF}(\mathbf{y}^S) = \int d\omega \left| \sum_{\mathbf{x}_r} \overline{\hat{P}(\mathbf{x}_r, \omega)} \hat{G}_0(\mathbf{x}_r, \mathbf{y}^S, \omega) \right|^2, \quad \hat{G}_0(\mathbf{x}, \mathbf{y}, \omega) = \frac{e^{i\omega\tau(\mathbf{x}, \mathbf{y})}}{4\pi|\mathbf{x} - \mathbf{y}|}$$

that is widely used in sonar and elsewhere in more general situations (waveguides, enclosures, etc) with a suitable \hat{G}_0 .

Decoherence distance X_d and decoherence frequency Ω_d

The trace cross-correlation

$$P(\mathbf{x}_r, \cdot) *_t P(\mathbf{x}_{r'}, -\cdot)(t)$$

does not have a peak if $|\mathbf{x}_r - \mathbf{x}_{r'}| > X_d$.

The phases of $\hat{P}(\mathbf{x}_r, \omega_1)$ and $\hat{P}(\mathbf{x}_r, \omega_2)$ decorrelate when $|\omega_1 - \omega_2| > \Omega_d$.

Both X_d and Ω_d can be **ESTIMATED** from the array data directly.

Coherent interferometric imaging

Use the Coherent Interferometric imaging functional:

$$I^{CINT}(\mathbf{y}^S; X_d, \Omega_d) = \int \int_{|\omega_1 - \omega_2| \leq \Omega_d} d\omega_1 d\omega_2 \sum \sum_{|\mathbf{x}_r - \mathbf{x}'_r| \leq X_d} \hat{P}(\mathbf{x}_r, \omega_1) \overline{\hat{P}(\mathbf{x}'_r, \omega_2)} e^{-i(\omega_1 \tau(\mathbf{x}_r, \mathbf{y}^S) - \omega_2 \tau(\mathbf{x}'_r, \mathbf{y}^S))}$$

If we take $X_d = a$ and $\Omega_d = B$, which means that there is no smoothing, then the CINT functional is just the Kirchhoff migration functional squared: $I^{CINT} = (I^{KM})^2$. The case $\Omega_d = 0$, suitably interpreted, is incoherent interferometry.

Adaptive Selection of X_d and Ω_d

For CINT to be effective we need to be able to determine the decoherence length and frequency **adaptively**. We do this by minimizing the bounded variation norm of the (random) functional I^{CINT}

$$\{X_d^*, \Omega_d^*\} = \operatorname{argmin}_{X_d, \Omega_d} \|I^{CINT}(\cdot; X_d, \Omega_d)\|_{BV}$$

where

$$\|f\|_{BV} = \int |f(\mathbf{y})| d\mathbf{y} + \alpha \int |\nabla f(\mathbf{y})| d\mathbf{y}$$

The bounded variation norm is used because it is smoothing on small scales but is respectful of large scale features (discontinuities). The smoothing is limited by the L^1 norm. Other sparsity-type norms can be used, such as entropy norms.

What about denoising the data first and then migrating?

The array data P , not the image, could be denoised by minimizing

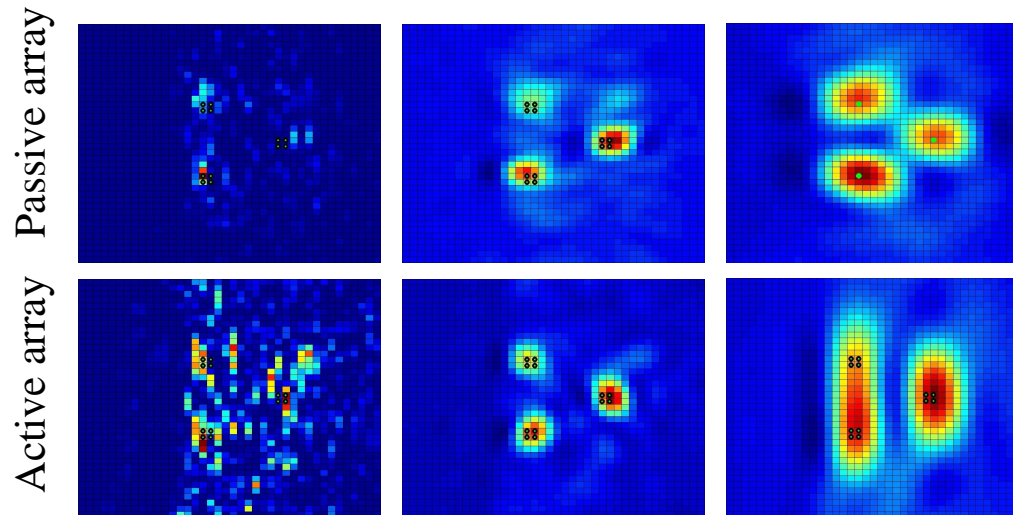
$$\alpha \|P - Q\|_{PROX} + \|Q\|_{REG}$$

over Q . This is an expensive calculation for large array data sets.

The denoising can also be done by harmonic analysis methods: decompose the data P in some well chosen basis (ridgelets?), threshold the Fourier coefficients below some level and reconstruct to get the denoised data Q .

After the denoising one can do Kirchhoff migration with Q as array data.

Coherent interferometric imaging results



Coherent Interferometry images in random media with $s = 3\%$.

Left Figures: $X_d = a$, $\Omega_d = B$ (Kirchhoff Migration, no smoothing)

Middle Figures: $X_d = X_d^*$, $\Omega_d = \Omega_d^*$ (Adaptively selected optimal smoothing)

Right Figures: $X_d < X_d^*$, $\Omega_d < \Omega_d^*$ (Too much smoothing)

Comments on the CINT results

- Without smoothing there is no statistical stability of the image: Different realizations of the random medium give different images. Smoothing, especially in frequency, gives stable but blurred images.
- Statistical stability of the image is very important because it allows further processing with deblurring methods. We have used **Level Set Deblurring** methods successfully, provided that we have a good estimate of the amount of blurring.
- The optimal decoherence frequency Ω_d^* is not known and it is determined adaptively, as explained above. So is the decoherence distance X_d^* .

Resolution theory for specific models

A resolution theory can be developed based on several assumptions about the random medium and the propagation regime.

Such assumptions are NOT used in the numerical simulations.

- With the paraxial approximation, the white noise limit, and a high frequency expansion we reduce all theoretical calculations to the use of one relatively simple formula obtained from the random Schrödinger equation: a second order moment formula.
- One other regime where analytical results can be obtained: Layered media. In no other regime do we have, or expect, analytical results.

Summary: Resolution limits

	Deterministic	Known Rand (TR)	Unknown Rand (CINT)
Range	$\frac{c_0}{B}$	$\frac{c_0}{B}$	$\frac{c_0}{\Omega_d}$
Cross Range	$\frac{c_0 L}{\omega a}$	$\frac{c_0 L}{\omega a_e} \sim X_d$	$\frac{c_0 L}{\omega X_d} \sim a_e$

Resolution limits in deterministic media and in random media, when the random medium is known as in physical time reversal, and when the random medium is not known as in coherent interferometry.

Role of coherence in array imaging

Coherence is essential in array imaging. A more physical, and more conventional, way to measure coherence is through the **transport mean free path** l^* . In the regime where waves energy propagates by diffusion, the diffusion coefficient is given by

$$D = \frac{c_0 l^*}{3}.$$

If the transport mean free path l^* is small compared to the range L of the object to be imaged then migration methods, including CINT, will not work. In our numerical simulations l^* is of the order of L , which is the regime where we expect CINT to be effective.

Optimal illumination and waveform design

Optimal illumination in array imaging is up to now aimed at **DETECTION**. That is, if $\hat{f}(\mathbf{x}_s, \omega)$ is the signal in the frequency domain that is emitted at \mathbf{x}_s then the signal received at \mathbf{x}_r is given by

$$\sum_{s=1}^{N_s} \hat{\Pi}(\mathbf{x}_r, \mathbf{x}_s, \omega) \hat{f}(\mathbf{x}_s, \omega).$$

The total power received at the array is given by

$$\mathcal{P} = \int_{|\omega - \omega_0| \leq B} d\omega \sum_{r=1}^{N_r} \left| \sum_{s=1}^{N_s} \hat{\Pi}(\mathbf{x}_r, \mathbf{x}_s, \omega) \hat{f}(\mathbf{x}_s, \omega) \right|^2.$$

We want to maximize this functional over all illumination signals $\hat{f}(\mathbf{x}_s, \omega)$ with the normalization

$$\int_{|\omega - \omega_0| \leq B} d\omega \sum_{s=1}^{N_s} \left| \hat{f}(\mathbf{x}_s, \omega) \right|^2 = 1$$

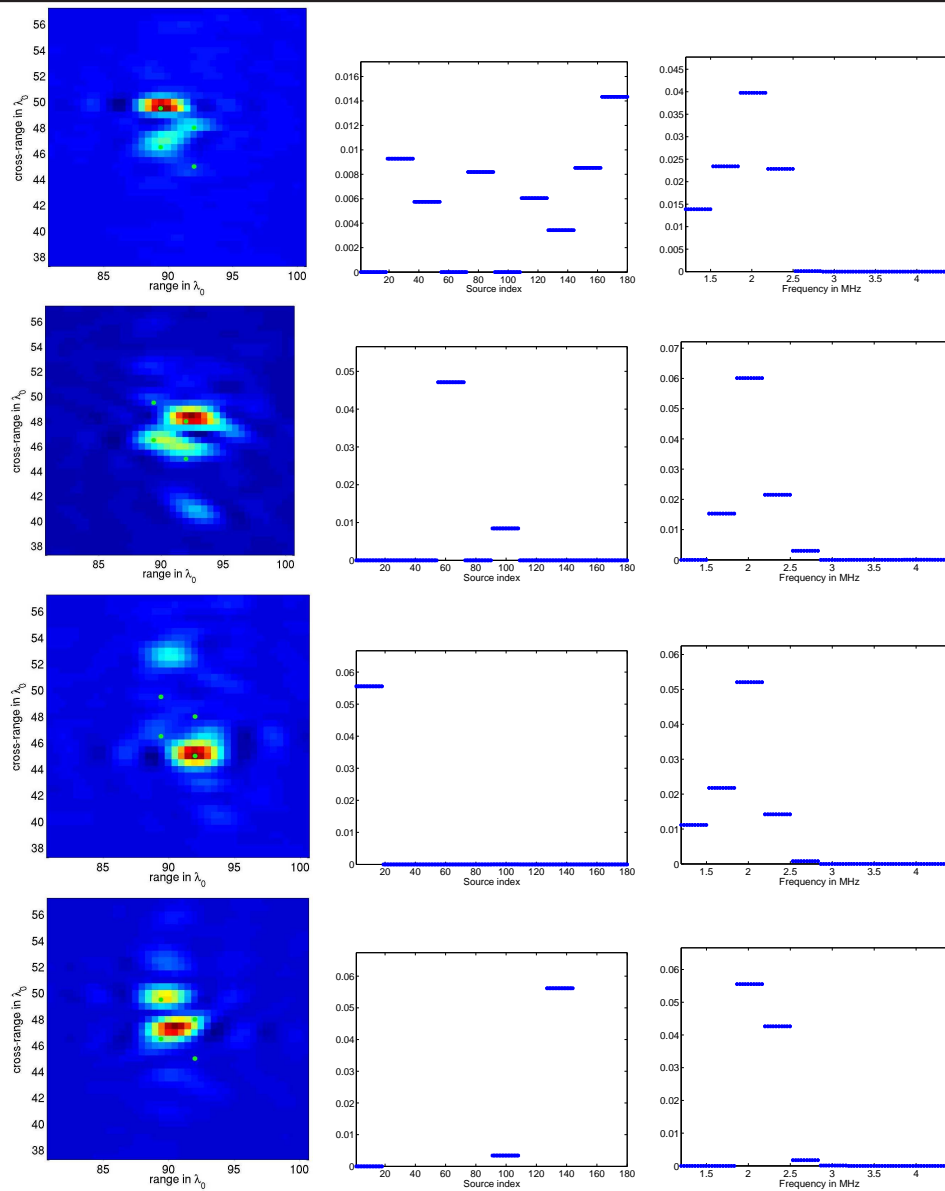
Optimal illumination and waveform design

In general, Optimal Illumination for Detection (SVD) produces images with bad resolution.

Just like in **Adaptive Coherent Interferometry** we can, however, introduce an optimal illumination objective that is tied to the resolution of the image itself.

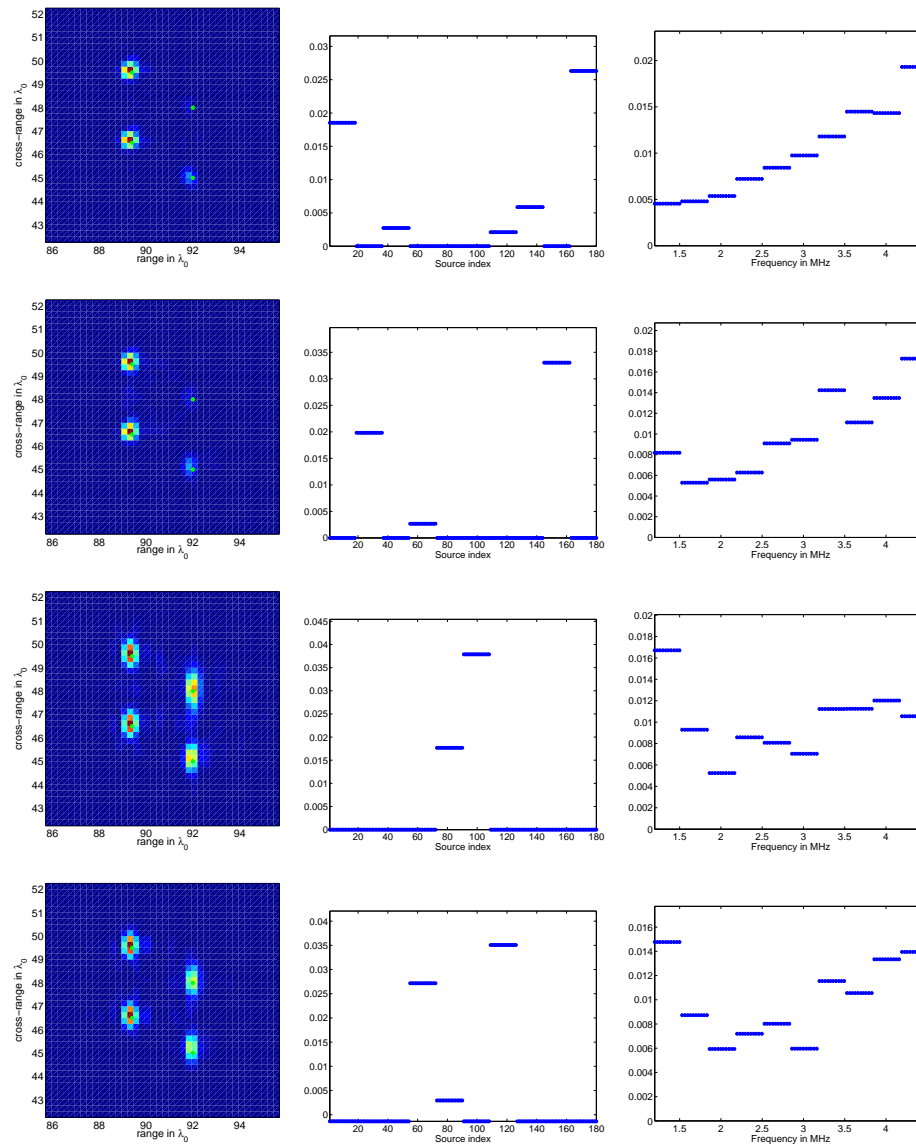
We now show the results of numerical simulations using this approach to optimal illumination.

Optimal Illumination, Random Medium



Left: image; Center, weights; Right: pulse.

Optimal Illumination, Deterministic Medium



Left: image; Center: weights; Right: pulse

The algorithm

We compute first the weighted average of the migrated traces

$$\widehat{m}(\mathbf{x}_r, \mathbf{y}^S, \omega) = \sum_{s=1}^{N_s} w_s \widehat{f}_B(\omega - \omega_0) \widehat{\Pi}(\mathbf{x}_r, \mathbf{x}_s, \omega) e^{-i\omega [\tau(\mathbf{x}_r, \mathbf{y}^S) + \tau(\mathbf{x}_s, \mathbf{y}^S)]}.$$

We then cross correlate these migrated traces

$$\begin{aligned} \mathcal{I}^{\text{CINT}}(\mathbf{y}^S; \mathbf{w}, \widehat{f}) &= \int_{|\omega - \omega_0| \leq B} d\omega \int_{\substack{|\omega' - \omega_0| \leq B \\ |\omega' - \omega| \leq \Omega_d}} d\omega' \\ &\sum_{r=1}^{N_r} \sum_{\substack{r'=1 \\ |\mathbf{x}_r - \mathbf{x}'_r| \leq \frac{2c_0}{(\omega + \omega')\kappa_d}}}^{N_r} \widehat{m}(\mathbf{x}_r, \mathbf{y}^S, \omega) \overline{\widehat{m}(\mathbf{x}_{r'}, \mathbf{y}^S, \omega')}, \end{aligned} \quad (1)$$

where $\mathbf{w} = (w_1, \dots, w_{N_s})$.

The algorithm, continued.

We determine \mathbf{w} and \hat{f} by minimizing an objective function $\mathcal{O}(\mathbf{w}, \hat{f})$ that quantifies the quality of the image. We take it to be the L^1 norm. We then determine the weights $\mathbf{w} = (w_1, \dots, w_{N_s})$ and the waveform $\hat{f}(\omega)$ as minimizers of $\mathcal{O}(\mathbf{w}, \hat{f})$, subject to the following constraints.

The weights should be nonnegative and sum to one

$$\sum_{s=1}^{N_s} w_s = 1, \quad w_s \geq 0, \quad s = 1, \dots, N_s. \quad (2)$$

The support of $\hat{f}(\omega) = \hat{f}_B(\omega - \omega_0)$ is restricted to the fixed frequency band $[\omega_0 - B, \omega_0 + B]$, we ask that

$$\hat{f}_B(\omega - \omega_0) \geq 0, \quad \text{for all } \omega \in [\omega_0 - B, \omega_0 + B] \quad (3)$$

and its integral is one.

Optimal subspace selection and CINT

Another way to introduce an optimization process using the SVD is by subspace selection. Let

$$D \left[\hat{\Pi}(\omega); \omega \right] = \sum_{j=1}^p \sigma_j(\omega) d_j(\omega) \hat{\mathbf{u}}_j(\omega) \hat{\mathbf{v}}_j^*(\omega)$$

a subspace selector with weights $\{d_j(\omega)\}$. Now let

$$m(\mathbf{x}_r, \mathbf{x}_s, \mathbf{y}^S, \omega; d) = D \left[\hat{\Pi}(\omega); \omega \right]_{rs} e^{-i\omega(\tau(\mathbf{x}_r, \mathbf{y}^S) + \tau(\mathbf{x}_s, \mathbf{y}^S))}$$

The CINT imaging functional to be optimized is:

$$I^{CINT}(\mathbf{y}^S; d) = \int \int_{|\omega - \omega'| \leq \Omega_d} d\omega d\omega' \sum_{|\mathbf{x}_r - \mathbf{x}_{r'}| \leq X_d} \sum_{|\mathbf{x}_s - \mathbf{x}_{s'}| \leq X_d} m(\mathbf{x}_r, \mathbf{x}_s, \mathbf{y}^S, \omega; d) m(\mathbf{x}'_r, \mathbf{x}'_s, \mathbf{y}^S, \omega'; d)$$

Summary of CINT and imaging in random media

- Coherent interferometry, which is the back propagation of **local** cross-correlations of traces, deals well with partial loss of coherence in cluttered environments.
- **Adaptive estimation** of the space-frequency decoherence addresses well the issue of **learning** the unknown environment.
- The key parameters Ω_d and X_d , which characterize the clutter, play a triple role: they are thresholding parameters for CINT, they determine its resolution, and characterize the coherence of the data. **Theory** and implementation issues merge.
- In **Optimal Subspace and Illumination** selection is computationally intensive but makes a huge difference.

Conclusions

Imaging in its many forms is at the center of modern applied mathematics.

- It is naturally interdisciplinary
- It is profoundly mathematical
- It has to deal with large data sets
- It has to deal with statistical issues
- It has to deal with optimization issues

Background References

1. 3D Seismic Imaging, B.L. Biondi, no 14 in Investigations in Geophysics (Tulsa: Society of Exploration Geophysics). Recent book on basic seismic imaging with detailed treatment of velocity analysis
2. Mathematics of Multidimensional Seismic Imaging, Migration, and Inversion, Bleistein N, Cohen J K and Stockwell J W Jr, Springer, 2001. Mathematical treatment of migration imaging
3. Wave propagation and time reversal in randomly layered media, Fouque, Garnier, Papanicolaou and Solna, Springer, 2007. The first five chapters cover basic wave propagation in layered media. Chapter 6 is a self-contained treatment of asymptotics for stochastic equations as it is used in the rest of the book. Chapter 7 is a basic, mathematical treatment of waves in one-dimensional random media
4. Wave propagation and scattering in the heterogeneous Earth, Sato H and Fehler M 1998 (New York: Springer-Verlag). The use of radiative transport in seismology
5. Transport equations for elastic and other waves in random media, Ryzhik L V, Papanicolaou G C and Keller J B, 1996, Wave Motion, vol 24, 327-370. A more mathematical treatment of topics found in the previous reference
6. Imaging the Earth's interior, Claerbout J F, 1985, (Palo Alto: Blackwell Scientific Publications). Introduction to migration imaging

References specific to the Lectures

1. Theory and applications of time reversal and interferometric imaging, Borcea, Papanicolaou and Tsogka, *Inverse Problems*, vol 19, (2003), pp. 5139-5164. Contains details of many calculations in the slides (Lectures II,III, VII,VIII)
2. Statistical stability in time reversal, Papanicolaou, Ryzhik and Solna, *SIAM J. on Appl. Math.*, 64 (2004), pp. 1133-1155. Contains details on calculations in Lectures VII-VIII
3. Self-averaging from lateral diversity in the Ito-Schroedinger equation, George Papanicolaou, Leonid Ryzhik and Knut Solna, *SIAM Journal on Multiscale Modeling and Simulation*, vol 6, (2007), pp. 468-492. Contains details (more mathematical) of lectures VII-VIII
4. Imaging and time reversal in random media, Liliana Borcea, Chrysoula Tsogka, G. Papanicolaou and James Berryman, *Inverse Problems*, 18 (2002), pp. 1247–1279. Use of SVD in imaging as in Lecture V
5. Edge illumination and imaging of extended reflectors, Liliana Borcea, George Papanicolaou and Fernando Guevara Vasquez, *SIAM Journal on Imaging Sciences*, vol 1 (2008), pp. 75-114. Use of SVD in edge illumination and imaging as in Lecture VI
6. Passive Sensor Imaging Using Cross Correlations of Noisy Signals in a Scattering Medium, Josselin Garnier and George Papanicolaou in: <http://math.stanford.edu/~papanico>. The paper on which Lecture IV is based, as well as the Lecture of Garnier

References specific to the Lectures, continued

- 7 Stable iterative reconstruction algorithm for nonlinear travel time tomography Berryman J, 1990, Inverse Problems, vol 6, 21-42. Basic reference for travel time tomography
- 8 Adaptive interferometric imaging in clutter and optimal illumination Borcea, Papanicolaou, and Tsogka, 2006, Inverse Problems, vol 22, 1405-1436. Paper on which Lectures IX and X are based, plus Tsogka's lectures
- 9 Optimal illumination and waveform design for imaging in random media Borcea, Papanicolaou, and Tsogka, 2007, J. Acoust. Soc. Am., vol 122, 3507-3518. Same as previous reference

References, on Green's function from cross correlations

1. Surface wave tomography from microseisms in Southern California, Sabra K G, Gerstoft P, Roux P, and Kuperman W, 2005, Geophys. Res. Lett., vol 32, L14311
2. Interferometric daylight seismic imaging, Schuster G T, Yu J, Sheng J and Rickett J, 2004, Geophysical Journal International, vol 157, 832-852
3. Velocity inversion by differential semblance optimization, Symes W W and Carazzone J J, 1991, Geophysics, vol 56, 654-663
4. Green's function representations for seismic interferometry, Wapenaar K and Fokkema J, 2006, Geophysics, vol 71, SI33-SI46
5. Surface-wave array tomography in SE Tibet from ambient seismic noise and two-station analysis I. Phase velocity maps, Yao H, van der Hilst R D, and de Hoop M V, 2006, Geophysical Journal International, vol 166, 732-744
6. Ambient noise cross correlation in free space: Theoretical approach, Roux P, Sabra K G, Kuperman W A, and Roux, A 2005, J. Acoust. Soc. Am., 117, 79-84

References for cross correlations, continued

- 7 Acoustic daylight imaging via spectral factorization: Helioseismology and reservoir monitoring, Rickett J and Claerbout J, 1999, The Leading Edge, vol 18, 957-960
- 8 Correlation of random wave fields: an interdisciplinary review, Larose E, Margerin L, Derode A, Van Tiggelen B, Campillo M, Shapiro N, Paul A, Stehly L, and Tanter M, 2006, Geophysics, vol 71, SI11-SI21
- 9 Seismic interferometry - turning noise into signal, Curtis A, Gerstoft P, Sato H, Snieder R, and Wapenaar K, 2006, The Leading Edge, vol 25, 1082-1092